Iranian Journal of Organic Chemistry Vol. 14, No. 3 (2022) 3385-3395

Wood-ash (WA): a highly efficient biocatalyst for the synthesis of α-amino nitrile derivatives using one-pot multicomponent reaction

Rezvaneh Rostamian, Daryoush Zareyee and Mohammad A. Khalilzadeh*

Department of Chemistry, Qaemshahr Branch, Islamic Azad University, Qaemshahr, Iran

Received: May 2022; Revised: May 2022; Accepted: July 2022

Abstract: Research on heterogeneous catalysts with characteristics such as recyclability, insolubility, and easy separation has been recently advanced by green chemistry. Wood ash, with high amounts of the abovementioned metal oxides, seems a suitable alternative used in reactions that need base catalysts. To synthesize α-aminonitrile benzofuran, the 2,4-hydroxyacetophenone and isopropenyl acetylene was mixed and stirred in the presence of Water Extract of Wood Ash (WEWA) catalyst, followed by the addition of amine derivatives and stirring over a 15-minute period. The addition of trimethylsilyl cyanide and its stirring for another 120 minutes were the next steps. Various natural resources were used to prepare several wood ash catalysts using different combustion temperatures. FT-IR, SEM, TEM, and XRD methods were utilized to characterize the catalysts. The catalytic efficacy of the resulting catalysts was examined in synthesizing derivatives of α-amino nitrile. As shown by the experimental results, the preparation of the catalysts at a temperature of 850 °C effectively promoted the multicomponent synthesis of α-amino nitrile derivatives in aqueous media, leading to significantly great productivity.

Keywords: α-amino nitrile benzofuran, Multicomponent reaction, Wood ash.

Introduction

The catalyst is the key to chemical conversions, and most industrial syntheses and almost all chemical reactions require a catalyst [1]. A catalyst reduces the activation energy to perform the reaction and thus increases the reaction rate. In general, catalysts are divided into homogeneous and heterogeneous categories based on the density state. Although homogeneous catalysts have several advantages such as 1) higher activity than the heterogeneous ones due to high dispersion in the reaction medium, 2) increased collision of raw material molecules with the catalyst due to greater mobility of the catalyst, 3) the use of smaller amounts of catalysts for catalysts reaction because the molecules of the reactants can approach the active centers of the catalyst from any direction, and 4) lower prices than heterogeneous catalysts [2],they show some major problems, including separation of the dissolved catalyst from the resulting mixture after the reaction completion, which may be challenging, particularly in the case of toxic catalysts, as failure in its removal can lead to environmental pollution. However, the phase of heterogeneous catalysts differs from that of the reactant, and unlike the other type, they are easily separated from the reaction mixture by spending less time and materials, with no product impurities. Besides, high temperature is another advantage of this catalyst [3]. Over the past few decades, catalysts and catalytic reactions have attracted much attention, especially in the chemical and pharmaceutical industries. In the pharmaceutical industry, for example, metal scraps need to be completely eliminated. Therefore, research on the development of a heterogeneous recyclable catalyst system has increased [4-8]. Green chemistry includes providing

*Corresponding author. E-mail: khalilzadeh73@gmail.com

scientific and basic methods to maintain health, environmental safety, and economy in chemical processes. The optimum application of catalysts, better performance of chemical reactions using non-toxic catalysts, and the design and development of ideal catalysts are among the principles of green chemistry. Chemical reactions, actually, require acidic or alkaline catalysts to accelerate. The use of strong acids such as H_2SO_4 and strong bases such as NaOH, causes many by-products to form in the reaction due to their high strength, because of which milder catalysts are more suitable [9, 10]. Multicomponent reaction (MCR) is an efficient method to practically construct various heterocyclic compounds within a single process while ensuring diverse and complex structures from uncomplicated and economical starting materials by generating different bonds in single synthetic operations [11]. Research has currently paid much attention to multicomponent reactions because they are simple, reduce waste production, need a shorter time for reaction, represent step/atom efficiency, require fewer steps for intermediate purification and mild reaction conditions, while they are also environmentally friendly [12]. Strecker reactions, whose discovery goes back to 1850, are the first MCRs with great importance, particularly from the perspective of life sciences. The coupling of three components (a carbonyl compound which is usually an aldehyde, an amine, alkaline metal, or hydrogen cyanide) and the production of α-amino nitriles result from Strecker reactions [13]. Strecker reactions are among the simplest and most effective techniques used to synthesize α-amino nitriles as significantly beneficial synthons for preparing α-amino acids and heterocyclic compounds, including imidazole and different molecules with biological importance. The contribution of α-Amino acids is significant both biologically and economically as they are widely used in chemical and biological fields [14]. For instance, α-Amino acids play an important role as precursors in protein synthesis while also contributing to pharmaceutical industries as chiral building blocks [15]. Wood ash (WA) is a waste generated by the combustion of wood and wood products. It is a highly alkaline mineral-organic compound that contains various elements, including calcium, potassium, magnesium, manganese, phosphorus, and sodium, as well as compounds containing SiO_2, Al_2O_3, and Fe_2O_3. Wood ash has the acidic character of Lewis due to its abundant alkali and alkaline earth metals, alkaline properties, and the presence of various metal oxides. It can act as a catalyst that plays both acidic and alkaline roles in improving and increasing the efficiency of many reactions [16, 41-45]. The alkaline nature of wood ash activates nucleophiles and the acidic nature activates electrophiles during a chemical reaction, increasing the rate and efficiency of reactions [17]. The physicochemical properties of this material are highly variable and important in determining its useful applications. These characteristics depend on factors such as tree species, tree growth area, combustion conditions and temperatures, other fuels used along with wood fuel, and wood ash collection methods. For example, hardwood produces more ash compared to softwood. As a result, more ash is produced by the tree bark and leaves compared to the inner wood parts [18]. As a result, about 0.4-1.2% of the weight used would turn into ash according to the wood type burnt [19]. According to numerous studies [20], calcium, with the highest abundance in wood ash, has similar features to agricultural lime. Besides, ash can be considered an adequate source of potassium, phosphorus, and magnesium [21], which is an excellent source of plant nutrients and can be used as agricultural fertilizer [22].The total amount of metals in WA indicates that this ash has a high potential for use as a catalyst in a variety of chemical transformations [23]. However, with the exception of a limited number of new studies focusing on biodiesel and esterification, research in this area is limited, and none has concentrated on WA as a heterogeneous catalyst for organic reactions [24].

Today, the economics and cost-effectiveness of a method may not be enough for a chemist. The recyclability of raw materials and biocompatibility of methods, the safety of products, the application of green rather than toxic solvents, the application of mild conditions, and the use of inexpensive reagents are some of the most attractive methods for development, providing simple and green methods to synthesize organic compounds [25]. For instance, water can be a cheap green solvent accelerating the organic reaction rates in the synthesis of various compounds. An interesting method to obtain α-amino nitriles is the Strecker reaction of various amines, ketones and Trimethylsilyl cyanide when a variety of homogeneous and heterogeneous catalysts are present, including $Yb(OTf)_3$ [26], $Pr(OTf)_3$ [27], $Cu(OTf)_2$ [28], $ZrCl_4$ [29], $BiCl_3$ [30], polymer-supported scandium triflate [31], montmorillonite [32], MCM-41 anchored sulphonic acid [33], nano powder TiO_2 P_{25} [34], sulfamic acid-functionalized magnetic Fe_3O_4 nanoparticles [35], K_2PdCl_4 [36],

heteropoly acid [37], xanthan sulfuric acid [38], and poly(4-vinyl pyridine)-SO_2 complex [39]. Although several new methods have been reported for the preparation of these compounds, many of them have major disadvantages such as the need to use toxic solvents, high reaction time, disposable catalysts, and so on. As a result, the development of green, cheap, and efficient catalysts for the production of benzochrome is very desirable [40].

The current paper aimed to prepare wood ash from various sources and use it in some organic reactions. Accordingly, ash samples from Russian olive (ROA), pine (PiA), and poplar (PoA) were prepared using the furnace method at different temperatures. According to the results of various analyses such as FT-TR, SEM, EDX, TEM, XRD, XRF, etc., we found that Russian olive ash obtained by high-temperature water extraction method had the best conditions and characteristics to use. The catalytic performance of this compound was evaluated using various reactions, including the synthesis of chiral derivatives of α-amino nitrile benzofuran by the four-component reaction of 4,2-dihydroxyacetophenone, isopropenyl acetylene, amine, and trimethylsilyl cyanide (scheme 1). We also tested the three-component reaction of 2-hydroxyacetophenone, amine, and trimethylsilyl cyanide when different amounts of catalyst were present by cyanosylationing the Schiff intervals (Scheme 2). According to the results, this catalyst performed very well compared to other acidic and basic catalysts. The structure of the synthesized compounds was confirmed using conventional FT-IR spectroscopy, NMR, Mass, and elemental analysis methods. Also, after synthesis, separation, and identification of the desired compounds, the biological activities, including antioxidant, antimicrobial, and antifungal of some synthesized derivatives, were evaluated while also comparing the inhibitory effects of these derivatives with the results of control such as vitamin C.

Results and discussion

Characterization of the WEWA

Basicity. We initially measured basicity to find the optimal conditions, coming to the conclusion that basicity was significantly affected by the wood sources and combustion temperatures. Thus, all samples of wood ash, produced under various temperatures of burning, underwent pH measurements, the results of which were shown in Table 1. As evidence shows, the effects of the wood sources and combustion temperatures on WA pH or basicity were confirmed. It was also shown that ROA had a significantly higher pH compared to ashes from pine (PiA) and poplar (PoA), while there was an increase in the burning temperature with an increase in the ash pH. As an instance, when the pH of pine ash changed from 9.45 to 11.65, the temperature increased from 450 to 850 °C, while higher temperatures (>850°C) led to a decrease in pH to 10.94. The greatest value of pH was obtained by ROA_{850}, which is possible due to CaCO3 (825 °C) thermal decomposition to CaO, leading to greater basicity as the temperature increases. This is, in turn, because CaO is more water-soluble compared to $CaCO_3$, resulting in higher basicity values [47]. However, a greatly stable silicate phase is formed through metal oxide (such as SiO_2 and CaO) interactions at temperatures >1000 °C, leading to a decrease in the pH, which is related to the lower water-solubility of the stable silicates [43, 48].

SEM–EDX analyses. The results of the ROA_{850} analyses are represented in Figure 2a, revealing the porosity, spongy morphology, rough surface, and the great surface area of the wood ash particles in this sample. The analyses led to the identification of several elements, including potassium (K), calcium (Ca), magnesium (Mg), phosphorus (P), oxygen (O), carbon (C), sulfur (S), aluminum (Al), silicon (Si), and sodium (Na). In line with our expectations, consistent dispersion of the C and O main elements was confirmed on the RO wood ash surface. besides, the EDX analyses and elemental mapping indicated C, K, Ca, Mg, and Si as the main resulting elements from ROA850 decomposition, confirming that calcium and potassium-rich carbonates and oxides were present on the RO wood ash surface (Figure **1**) [43].

XRD Technique. Figure 3 shows the XRD patterns related to the RO wood ash produced under various temperatures of combustion (450, 850, and 1050°C). As shown by ROA_{450} XRD patterns, CaCO3, SiO_2, Fe_2O_3, , KCl and $MgCO_3$ components were present in this sample. However, the XRD patterns of ROA_{850} showed that KCl, CaO, Fe_2O_3, MgO, $CaCO_3$, K_2SO_4, and $Ca_2SiO_4.0.05Ca_3(PO4)_2$ compounds were present in the sample. On the other hand, the results of ROA1050 analyses showed an increase in the peak numbers and intensities associated with $Ca_2SiO_4.0.05Ca_3(PO4)_2$, which was the main component (Figure 2) [43].

X-ray fluorescence (XRF). The mechanisms for the formation of mineral compounds ash by wood combustion are still unclear, even though such an

exchange seems to depend on the combustion temperature and present atmosphere. The results obtained from the chemical composition analyses of RO wood ash are presented in Table 1 for various burning temperatures (450, 850, and 1050 °C). The XRF analyses showed Na_2O, K_2O, MgO, BaO, CaO, SiO_2, Al_2O_3, $P2O_5$, Fe_2O_3, and MnO_2 as the minerals present in the wood ash. Table 1 shows modifications found in the RO wood ash compositions at different combustion temperatures at a range of 450-1050 °C. As shown by the XRD analyses of ROA_{850} in Figure 2, the combustion temperature of 850 °C leads to the increased content of Cao primarily due to $CaCo_3$ decay. Na_2O and MgO percentages would decrease by increasing the temperature, which is mainly because carbonates are decomposed to oxides and subsequently volatilized. Based on Eq.2, the percentage of potassium decreases primarily due to KCl vaporization. On the other hand, the increase in the content of CaO is probably due to CaO non-volatility from wood ash [43, 50-51].

$$CaCO_3 \longrightarrow CaO + CO_2 \quad (500\text{-}825\ ^\circ C) \quad \text{Eq. 1}$$

$$KCl\ (l) \longrightarrow KCl\ (g) \quad (900\text{-}1100\ ^\circ C) \quad \text{Eq. 2}$$

$$CaO + P_2O_5 + SiO_2 \longrightarrow CaSiO_4 + 0.05\ Ca_3(PO_4)_2 \quad \text{Eq. 3}$$

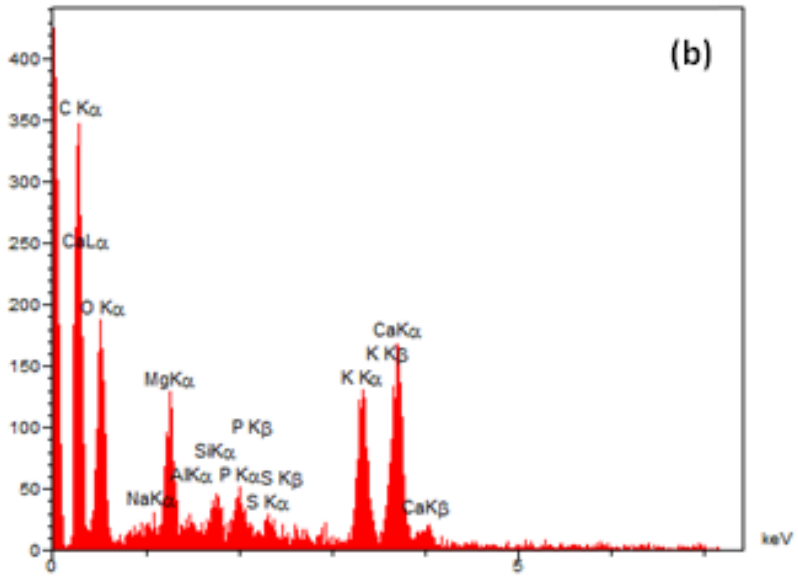

Figure 1. EDX elemental analysis of RO wood ash at 850 °C (ROA850)

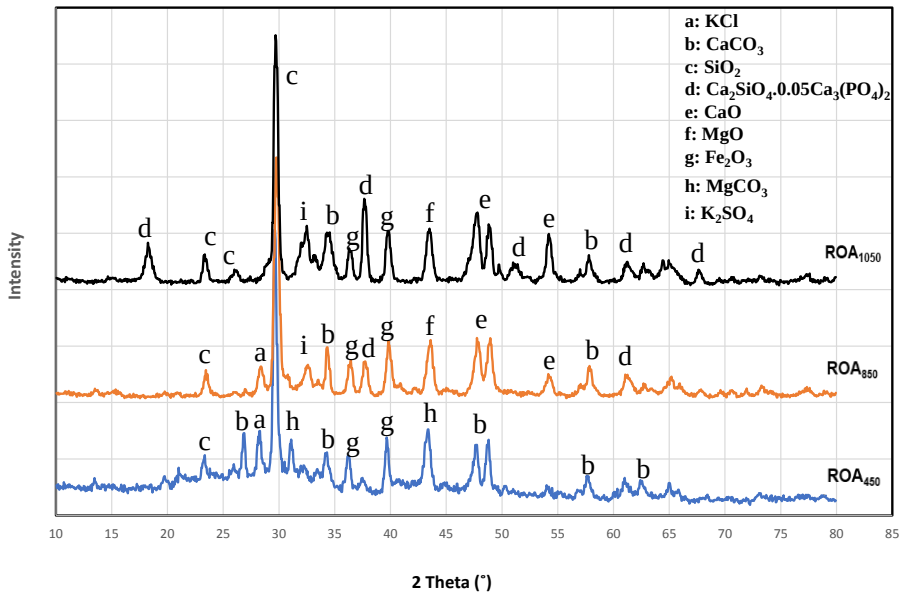

Figure 2. XRD pattern of WA at different combustion temperatures.

Table 1. Chemical composition of the WA from Russian olive in different combustion temperatures

Sample	Na_2O	K_2O	MgO	BaO	CaO	SrO	CuO	SiO_2	Al_2O_3	P_2O_5	Fe_2O_3	MnO_2	TiO_2	SO_3
ROA_{450}	0.7	20.6	7.4	1.7	45.6	1.6	–	7.2	1.6	4.3	3.6	0.3	0.2	5.2
ROA_{850}	0.5	14.5	9.64	0.2	61.5	2.1	0.1	2.9	0.51	2.5	0.9	0.3	0.1	4.3
ROA_{1050}	0.2	4.2	3.4	1.6	64.9	3.5	1.2	3.5	3.2	2.3	4.2	1.6	0.5	5.7

*FT-IR analyses. T*he FT-IR spectra related to the burnt samples of wood ash under temperatures of 450, 850, and 1050 °C. As observed in this figure, the broadband at 3453 cm^{-1} corresponds to hydroxyl stretching vibrations in some organic and inorganic components. Based on the available evidence, the increase in the temperature leads to a decrease in the intensity of absorbance because organic components burn. The week absorbance bands at 2922 and 2853 cm^{-1} from C-H stretching vibrations are associated with aliphatic hydrocarbons in wood ash, while the absorbance band at 1789 cm^{-1} and the shoulder on the XRD peak at 1621 cm^{-1} are associated with carbonyl and C=C groups, respectively. The absorbances around 1793, 1443, 876, and 712 cm^{-1} correspond to carbonate (CO_3^{2-}), while the characteristic bands at 1111, 1043, and 615 cm^{-1} for PO_4^{3-} and SiO_2 constituents represent metal carbonate carbonates such as $CaCO_3$, SiO_2, and metal phosphate. The absorbance bands at 1413, 1053, 523, and 471 cm^{-1} are observed in the wood ash FT-IR spectra under higher temperature ranges (ROA_{850} and R OA_{1050}), confirming that Si–O–Al, Si–O–Si, and CaO functionalities are present [43, 52-53].

Catalytic studies

To evaluate the catalytic performance of this compound, various reactions were carried out, including the synthesis of chiral derivatives of 4-amino nitrile benzofuran by the four-component reaction of 4,2-dihydroxyacetophenone, isopropenyl acetylene, amine, and trimethylsilyl cyanide and synthetamine. We tested the three-component reaction between 2-hydroxyacetophenone, amine, and trimethylsilyl cyanide using various catalyst quantities by cyanosylationing the Schiff intervals.

Synthesis of α-amino nitrile benzofurans (5a–f):

The current study investigated a green technique to prepare several derivatives of α-amino nitriles using a well-organized three-component reaction of 4,2-dihydroxyacetophenone **1**, isopropenylacetylene **2**, different amine **3** and trimethylsilyl cyanide **4**

whenROA_{850} catalytic quantities (%5) were present in 50 °C water with large yields (Scheme 3).

The condensation reaction of 4,2-dihydroxyacetophenone **1**, isopropenylacetylene **2**, methyl amine **3a,** and trimethylsilyl cyanide **4** was initially performed in 50 °C water to ensure the optimal reaction conditions considering the model reaction (Table 2).

According to the results in Table 2, the reaction was not performed at room temperature after about 15 hours (row 1) in the absence of the WEWA catalyst, and only a very small amount of product was formed after 15 hours by increasing the temperature in the absence of catalyst (Rows 2 and 3) and using strong hydroxide wire with different values of low reaction efficiency (rows 8, 9, and 10). The use of strong bases such as sodium hydroxide in a side reaction creates by-products and therefore reduces the production efficiency of the main reaction product. Different amounts of WEWA were used to optimize the catalyst (rows 4, 5, and 6). According to the current results, using 4 ml of WEWA (5%), the reaction proceeded with 99% efficiency (row 5). No significant effects on reaction efficiency were observed when higher amounts of catalyst were used. In fact, 4 ml of WEWA catalyst (5%) creates the best conditions for the reaction, forming the formed with 99% efficiency in 3 hours. Applying the lower values (1%) of the catalyst mentioned in row 4 has advanced the reaction with a yield of 55% in 2 hours. However, according to the molar ratios of the raw materials used, this amount of catalyst is low and the reaction stopped after 2 hours. An excessive increase in the amount of catalyst would lead to adverse economic effects and reduce the effective collisions between raw materials and by-products. The reaction temperature also declined according to the table below, indicating that the reaction efficiency is low at room temperature and increases by raising the temperature to about 50 ° C (row 5). As the temperature rises, the molecular motion increases, subsequently increasing the effective collisions between the raw materials, which will lead to the reaction. The reaction temperature also increased from 50 ° C to 90 ° C (row 7), which reduced the reaction efficiency. The rise in temperature, on the other hand, leads to unwanted reactions and the creation of by-products, while it can also cause the solvent to evaporate.

NaOH, which is a strong base, has a lower efficiency percentage than WEWA (5%) because the use of strong bases such as sodium hydroxide in a side reaction results in by-products and therefore reduces the production efficiency of the main reaction product.

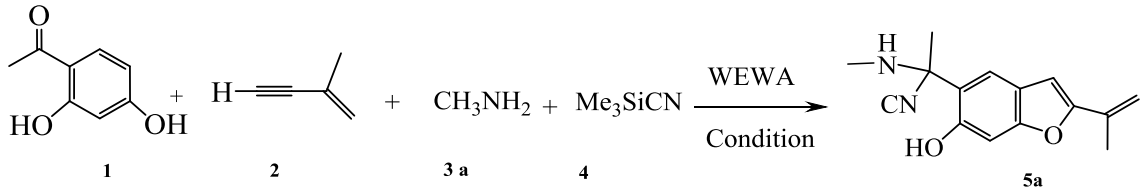

Scheme 3. Model reaction of 4,2-dihydroxyacetophenone **1**, isopropenylacetylene **2**, methyl amine **3a** and trimethylsilyl cyanide **4** for the synthesis of 5a in the presence of WEWA

Table 2. Screening the model reaction conditions of 4,2-dihydroxyacetophenone 1, isopropenylacetylene 2, methyl amine 3a, and trimethylsilyl cyanide 4 to synthesize 5a in the presence of WEWA.

Entry	Catalyst	Temp. (°C)	Time (h)	Yield %[a]
1	None	Rt	15	–
2	None	50	15	Trace
3	None	90	15	Trace
4	ROA_{850} (%1)	50	2	55
5	**ROA_{850} (%5)**	**50**	**3**	**99**
6	ROA_{850} (%10)	50	3	99

7	ROA_{850} (%5)	90	3	98
8	NaOH (%5)	50	5	48
9	NaOH (%10)	50	5	52
10	NaOH (%20)	50	5	51

[a] Isolated yield

FT-IR, ^{1}H NMR, ^{13}C NMR, and mass spectral data supported the compounds **5** structures (see supporting information for more details).

Mechanistically, it is possible that the reactions include the first formation of intermediate **8** from the 2,4-dihydroxyacetophenone **1** and isopropenylacetylene **2** reaction, taking place with primary amines **3** in the presence of a catalytic amount of WEWA and producing imines **9.** In the presence of the catalyst, nitrile negative ion (CN^-) from compound **4** attacks imines and produces product **5**. It should be mentioned that WEWA has Lewis acid and basic sites. In these reactions, the acid sites interact with the oxygen of the carbonyl group, and the basic site of WEWA helps to take up a proton to produce compound **5**. The method of reaching the final product 5 in the vicinity of the WEWA catalyst is shown in the following figure. WEWA catalyst removes protons from the hydroxyl group of compound number 1 due to its alkaline properties, de-protonizes this group, and increases its nucleophilicity. The phenoxy group, with a negative charge on the oxygen atom, is conjugated with the double bonds of the ring, and as a result of this resonance, the negative charge is placed on the carbon in the ortho position of the ring, and the carbon-oxygen bond is closed in a carbonyl form. The carbon of the ortho position of the carbonyl group (carbon α) has a negative charge, and this carbonyl attacks the triple bond as a nucleophile. Removal of the hydrogen of the hydroxyl group on the ring is done with the help of a catalyst. Furthermore, the WEWA catalyst removes protons from the amino group of compound number 3 due to its alkaline property and increases its nucleophilic property while activating the carbonyl group of compound number 10 and the property of electrons due to its acidic property. The electrophilic features increase and speed up the reaction of the two. Compound No. 3 with the unbonded electron pair of nitrogen atoms as nucleophiles attack the carbonyl group of Compound No. 10 and the double bond C = O is opened, and Compound No. 13 is formed by removing the water molecule. The C = N bond of the immune compound is subjected to the nucleophilic attack of the cyanide group of compound No. 4, and product No. 5 is formed (Scheme 4).

Asymmetric synthesis of α-amino nitriles (7a–d):

The reactions of 2-hydroxyacetophenone **6**, various amine **3,** and trimethylsilyl cyanide **4** were examined in similar conditions when ROA_{850} (%5) catalyst was present in aqueous media subject to a temperature of 50 °C to confirm the differences between the studied reactions. IR, ^{1}H NMR, ^{13}C NMR, and mass spectral data supported the compounds 7 structures.

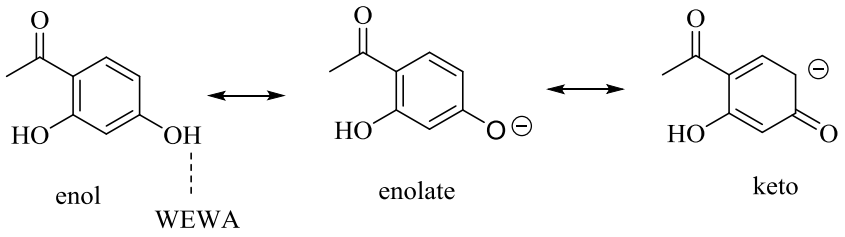

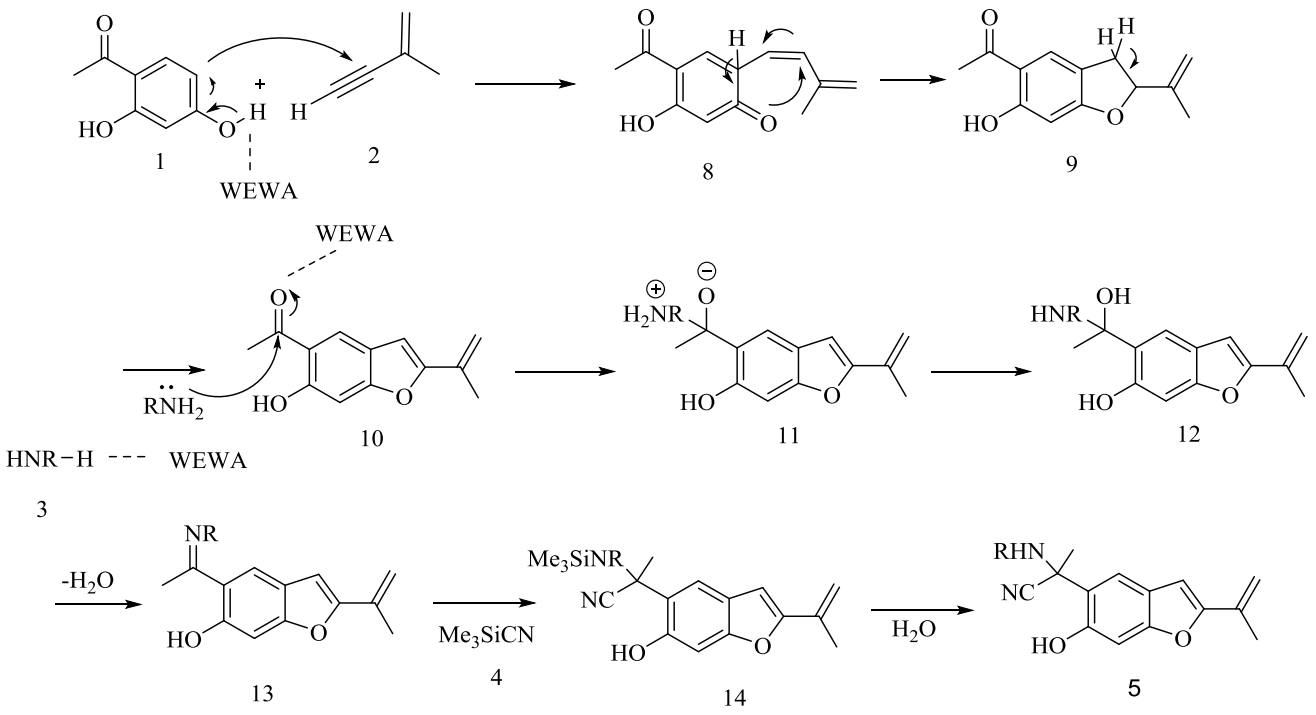

Scheme 4. Proposed mechanism for the synthesis of α-amino nitrile benzofuranes 5

Conclusions

Wood ash (WA) is a waste generated by the combustion of wood and wood products. This residue is a potential inorganic-organic compound and has both alkaline and acidic properties with its abundant alkaline, alkaline earth metals, and various metal oxides. It can also act as a heterogeneous catalyst, effectively enhancing electrophilic and nucleophilic activities and increasing the efficiency and speed of reactions. Physical and chemical properties of wood ash are important in determining its useful applications, while factors such as tree species, tree growth area, combustion conditions, temperature, other fuels used with wood fuel, and wood ash collection method also play a significant role. Considering the high potential properties and practical applications of this compound, we decided to study the elemental, molecular, and mineral composition of the ash from several types of wood and examine their catalytic activities. Various analyses, including FT-TR, SEM, EDX, TEM, XRD, and XRF, were also performed on the samples. According to the results, RO ash obtained by water extraction at high temperatures showed high acid-base properties compared to other samples of wood ash. Thus, pH analysis showed high pH, and XRF analysis showed large quantities of acidic compounds in the abovementioned sample. A multicomponent reaction was used to synthesize the chiral derivatives of benzofuran α-amino nitrile and asymmetric α-amino nitriles and investigate the catalytic efficiency of the compound. Besides, the IR, Mass, NMR, and CHNS spectroscopy methods supported the structure of the synthesized compounds. The benefits of the developed method in comparison with the previous ones include low price, easy preparation of the catalyst, high efficiency, the reaction in an acceptable time, easy separation of the catalyst from the reaction medium, environmentally friendly, and recovery and reuse of the catalyst. This catalyst is recommended for various reactions required to perform in acidic or alkaline environments.

Experimental Section

All chemicals were available commercially and used without additional purification. The catalyst was synthesized according to the literature. The FT-IR spectra of the products were obtained with KBr disks, using a Tensor 27 Bruker spectrophotometer. The ^{1}H NMR (400 and 500 MHz) spectra were recorded using Bruker 400 and 500 spectrometers.

General experimental procedure:

A mixture of dimedone **1** (1 mmol), aldehyde **2** (1 mmol), malononitrile **3** (1 mmol) and Fe_3O_4 MNPs

(0.09 g) as catalyst was heated in water for the appropriate time. The reaction was monitored by TLC. Upon completion of the transformation, hot ethanol was added and the catalyst filtered through sintered glass Büchner funnel under hot conditions. The catalyst was washed with a small portion of hot ethanol. After cooling, the combined filtrate was allowed to stand at room temperature. The precipitated solid was collected by filtration, and recrystallized from ethanol to give compounds **4** in high yields.

2-amino-7,7-dimethyl-5-oxo-4-phenyl-5,6,7,8-tetrahydro-4H-benzopyran-3-carbonitrile (4a):

^{1}H NMR (400 MHz, DMSO-d_6): δ 0.97 (s, 3H, CH_3), 1.05 (s, 3H, CH_3), 2.10 (d, 1H, *J* = 16.0 Hz, CH_2, diastereotopic proton), 2.27 (d, 1H, *J* = 16.0 Hz, CH_2, diastereotopic proton), 2.45–2.55 (m, 2H, CH2, diastereotopic protons overlapped with solvent), 4.18 (s, 1H, CH), 7.03 (s br., 2H, NH_2), 7.10–7.24 (m, 3H, arom-H), 8.16 (t, 2H, *J* = 7.2 Hz, arom-H); FT-IR (KBr disc): ν 3342, 3061, 2982, 1688, 1651, 1489, 1372, 1211, 1167, 828.

2-amino-4-(4-chlorophenyl)-7,7-dimethyl-5-oxo-5,6,7,8-tetrahydro-4H-benzopyran-3-carbonitrile (4b):

^{1}H NMR (500 MHz, DMSO-d_6): δ 0.95 (s, 3H, CH_3), 1.03 (s, 3H, CH_3), 2.10 (d, 1H, *J* = 16.0 Hz, CH_2, diastereotopic proton), 2.24 (d, 1H, *J* = 16.0 Hz, CH_2, diastereotopic proton), 2.45–2.55 (m, 2H, CH2, diastereotopic protons overlapped with solvent), 4.19 (s, 1H, CH), 7.05 (s br., 2H, NH_2), 7.17 (d, 2H, *J* = 8.4 Hz, arom-H), 7.34 (d, 2H, *J* = 8.4 Hz, arom-H); FT-IR (KBr disc): ν 3342, 3061, 2982, 1688, 1651, 1489, 1372, 1211, 1167, 828.

2-amino-4-(4-methoxyphenyl)-7,7-dimethyl-5-oxo-5,6,7,8-tetrahydro-4H-benzopyran-3-carbonitrile (4c):

^{1}H NMR (500 MHz, DMSO-d_6): δ 0.94 (s, 3H, CH_3), 1.04 (s, 3H, CH_3), 2.08 (d, 1H, *J* = 16.0 Hz, CH_2, diastereotopic proton), 2.24 (d, 1H, *J* = 16.0 Hz, CH_2, diastereotopic proton), 2.42–2.56 (m, 2H, CH2, diastereotopic protons overlapped with solvent), 3.71 (s, 3H, OCH_3), 4.12 (s, 1H, CH), 6.83 (d, 2H, *J* = 8.7 Hz, arom-H), 6.93 (s br., 2H, NH_2), 7.04 (d, 2H, *J* =8.7 Hz, arom-H); FT-IR (KBr disc): ν 3342, 3061, 2982, 1688, 1651, 1489, 1372, 1211, 1167, 828.

2-amino-7,7-dimethyl-4-(3-nitrophenyl)-5-oxo-5,6,7,8-tetrahydro-4H-benzopyran-3 carbonitrile (4d):

^{1}H NMR (500 MHz, DMSO-d_6): δ 0.96 (s, 3H, CH_3), 1.04 (s, 3H, CH_3), 2.11 (d, 1H, *J* = 16.1 Hz, CH_2, diastereotopic proton), 2.27 (d, 1H, *J* = 16.1 Hz, CH_2, diastereotopic proton), 2.55 (s, 2H, diastereotopic proton), 4.42 (s, 1H, CH), 7.17 (s br., 2H, NH_2), 7.55–7.50 (m, 2H, arom-H), 7.97 (t, 1H, *J* = 1.7 Hz, arom-H), 8.05–8.10 (m, 1H, arom-H); FT-IR (KBr disc): ν 3342, 3061, 2982, 1688, 1651, 1489, 1372, 1211, 1167, 828.

2-amino-4-(4-fluorophenyl)-7,7-dimethyl-5-oxo-5,6,7,8-tetrahydro-4H-benzopyran-3-carbonitrile (4e):

^{1}H NMR (400 MHz, DMSO-d_6): δ 0.96 (s, 3H, CH_3), 1.04 (s, 3H, CH_3), 2.11 (d, 1H, *J* = 16.2 Hz, CH_2, diastereotopic proton), 2.26 (d, 1H, *J* = 16.2 Hz, CH_2, diastereotopic proton), 2.41–2.55 (m, 2H, CH2, diastereotopic protons overlapped with solvent), 4.21 (s, 1H, CH), 7.07 (s br., 2H, NH_2), 7.08–7.23 (m, 4H, arom-H); FT-IR (KBr disc): ν 3342, 3061, 2982, 1688, 1651, 1489, 1372, 1211, 1167, 828.

2-amino-4-(4-bromophenyl)-7,7-dimethyl-5-oxo-5,6,7,8-tetrahydro-4H-benzopyran-3-carbonitrile (4f):

^{1}H NMR (400 MHz, DMSO-d_6): δ 0.96 (s, 3H, CH_3), 1.05 (s, 3H, CH_3), 2.11 (d, 1H, *J* = 16.0 Hz, CH_2, diastereotopic proton), 2.26 (d, 1H, *J* = 16.0 Hz, CH_2, diastereotopic proton), 2.45–2.55 (m, 2H, CH2, diastereotopic protons overlapped with solvent), 4.19 (s, 1H, CH), 7.10 (s br., 2H, NH_2), 7.12 (d, 2H, *J* = 8.4 Hz, arom-H), 7.50 (d, 2H, *J* = 8.4 Hz, arom-H); FT-IR (KBr disc): ν 3342, 3061, 2982, 1688, 1651, 1489, 1372, 1211, 1167, 828.

2-amino-4-(3-bromophenyl)-7,7-dimethyl-5-oxo-5,6,7,8-tetrahydro-4H-benzopyran-3-carbonitrile (4g):

^{1}H NMR (400 MHz, DMSO-d_6): δ 0.97 (s, 3H, CH_3), 1.05 (s, 3H, CH_3), 2.14 (d, 1H, *J* = 16.0 Hz, CH_2, diastereotopic proton), 2.27 (d, 1H, *J* = 16.0 Hz, CH_2, diastereotopic proton), 2.45–2.55 (m, 2H, CH2, diastereotopic protons overlapped with solvent), 4.22 (s, 1H, CH), 7.13 (s br., 2H, NH_2), 7.15–7.20 (m, 1H, arom-H), 7.20-7.35 (m, 2H, arom-H), 7.37–7.45 (m, 1H, arom-H); FT-IR (KBr disc): ν 3342, 3061, 2982, 1688, 1651, 1489, 1372, 1211, 1167, 828.

2-amino-7,7-dimethyl-5-oxo-4-(thiophen-2-yl)-5,6,7,8-tetrahydro-4H-benzopyran-3-carbonitrile (4h):

^{1}H NMR (400 MHz, DMSO-d_6): δ 0.99 (s, 3H, CH_3), 1.05 (s, 3H, CH_3), 2.15 (d, 1H, *J* = 16.2 Hz, CH_2,

diastereotopic proton), 2.31 (d, 1H, J = 16.2 Hz, CH_2, diastereotopic proton), 2.44 (d, 1H, J = 17.4 Hz, CH_2, diastereotopic proton), 2.56 (d, 1H, J = 17.4 Hz, CH_2, diastereotopic proton), 4.55 (s, 1H, CH), 6.87 (d, 1H, J = 2.8 Hz, arom-H), 6.92 (dd, 1H, J = 5.0, 3.4 arom-H), 7.15 (s br., 2H, NH_2), 7.40 (dd, 1H, J = 4.8, 0.8 Hz, arom-H); FT-IR (KBr disc): ν 3342, 3061, 2982, 1688, 1651, 1489, 1372, 1211, 1167, 828.

Acknowledgments

The authors thanks from their gratitude for its financial support.

References

[1] Augugliaro, V.; Palmisano, G.; Palmisano, L.; Soria, J. Heterogeneous Photocatalysis and Catalysis, Elsevier, CHAPTER 1, **2019**.
[2] Anastas P.; Eghbali, N. *Chem. Soc. Rev*., **2010**, *39*, 301.
[3] Rosowski, F. et al., *Handbook of Heterogeneous Catalysis*, Wiley-VCH, New York, **2008**.
[4] Chadwick, J. C. *Homogeneous Catalysts: Activity-Stability-Deactivation*, 1st edition, John Wiley & Sons, The Netherlands, **2011**.
[5] Khalilzadeh, M. A.; Hossaini, Z.; Baradarani, M. M.; Hasannia. A. *Tetrahedron* **2010**, *66*, 8464.
[6] Tajbakhsh, M.; Heydari, A.; Khalilzadeh, M. A.; Lakouraj, M. M; Zamenian, B.; Khaksar. S. *Synlett* **2007**, *15*, 2347.
[7] Khalilzadeh, M. A.; Arab., Z. *Curr. Anal. Chem.* **2017**, *13*, 81.
[8] Seyednejhad, S.; Khalilzadeh, M. A.; Zareyee, D.; Sadeghifar, H.; Venditti, R. *Cellulose* **2019**, *26 (8)*, 5015.
[9] Jiang, B.; Rajale, T.; Wever, W.; Tu, S. J.; Li, G. *Chem. Asian. J.*, **2010**, *523*, 2318.
[10] Ugi, I. *Pure Appl. Chem.*, **2001**, *73*, 187.
[11] Nair, V.; Rajesh; C.; Vinod, A. U.; Bindu, S.; Sreekanth, A. R.; Mathen J. S.; Balagopal L. *Acc. Chem. Res.* **2003**, *36*, 899.
[12] Ramón, D. J.; Yus, M. *Angew, Chem., Int. Ed.*, **2005**, *44*, 602.
[13] Strecker, A. *Ann. Chem. Pharm.* **1850**, *75(1)*, 27.
[14] Enders, D.; Shilvock, J. P. *Chem. Soc. Rev.* **2000**, *29(5)*, 359.
[15] Duthaler, R. O. *Tetrahedron*. **1994**, *50(6)*, 1539.
[16] Etiégni, L.; Campbell, A. G. *Bioresour. Technol.* **1991**, *37*, 173.
[17] Olanders, B.; Steenari, B. *Biomass Bioenergy* **1995**, *8*, 105.
[18] Aprianti, S. E. *J. Clean. Prod.* **2017**, *142*, 178.
[19] Werkelin, J.; Skrifvars, B. J.; Hupa, M. *Biomass Bioenergy* **2005**, *29*, 451.
[20] Erich, M. S.; Ohno, T. *Analyst* **1992**, *117*, 9.
[21] Ulery, L.; Graham, R. C.; Amrhein, C. *Soil Sci.* **1993**, *156*, 35.
[22] Gholipour, B. *Green. Chem.* **2021**, *23*, 6223.
[23] Al-Rahbi, S.; Williams, P. T. *J. Mater. Cycles Waste Manag.* **2019**, *21*, 1224.
[24] Deyris, P. A.; Adler, P.; Petit, E.; Legrand, Y. M.; Grison, C. *Green Chem.* **2019**, *21*, 3133.
[25] Miladinović, M. R.; *Renew. Energy* **2020**, *147*, 1033.
[26] Kobayashi, S.; Ishitani, H.; Ueno, M, *Synlett*, **1997**, 8, 115.
[27] De, S. K.; Gibbs, R. A.; *Synth. Commun.* **2005**, *35*, 961.
[28] Paraskar, S.; Sudalai, A. *Tetrahedron Lett.* **2006**, *47*, 5759.
[29] Raghu, M.; Reddy, C. S.; *Indian J. Chem*. **2009**, *48B*, 295.
[30] De, S. K.; Gibbs, R.;A.,*Tetrahedron Lett.* **2004**, *45*, 7407.
[31] Kobayashi, S.; Nagayama, S.; Busujima, T. *Tetrahedron Lett.* **1996**, *37*, 9221.
[32] Yadav, J. S.; Reddy, B. V. S.; Eeshwaraiah, B.; Srinivas, M. *Tetrahedron.* **2004**, *60*, 1767.
[33] Dekamin, M. G.; Mokhtari, Z., *Tetrahedron* **2012**, *68*, 922.
[34] Baghbanian, S. M.; Farhang, M.; Baharfar, R. *Chin. Chem. Lett*. **2011**, *22*, 555.
[35] Kassaee, M. Z.; Masrouri, H.; Movahedi, F. *Appl. Catal. A: Gen.* **2011**, *395*, 28.
[36] Karmakar, B.; Banerji, J.; *Tetrahedron Lett.* **2010**, *51*, 2748.
[37] Rafiee, E.; Rashidzadeh, S.; Joshaghani, R.; Chalabeh, H.; Afza, K. *Synth. Commun.* **2008**, *38*, 2741.
[38] Shaabani, A.; Maleki, A.; Soudi, M. R.; Mofakham, H. *Catal. Commun*. **2009**, *10*, 945.
[39] Olah, G. A.; Mathew, T.; Panja, C.; Smith, K.; Prakash, G. K. S.; *Catal. Lett.* **2007**, *114*, 1.
[40] Hajipour Najar, A.; Hossaini, Z.; Abdolmohammadi, Sh.; Zareyee. D. *Comb. Chem. High Throughput Scr*. **2020**, *23*, 345.
[41] Sharma, M.; Ali Khan, A.; Puri, S. K.; Tuli, D. K. *Biomass Bioenergy* **2012**, *41*, 94.
[42] Lopinti, K. *Catal. Lett.* **2020**, *150*, 1163.
[43] Rostamian, R.; Khalilzadeh, M. A.; Zareyee. D. Scientific Reports, **2020**, *12*, 1145.
[44] Lopinti, K.; Sharma, M.; Chakradhar, M.; Arora, A. K.; Kagdiyal, V.; Majumdar, S. K. *Catal. Lett.*, **2020**,*150*, 1163.
[45] Sharma, M.; Khan, A. A.; Puri, S. K.. Tuli, D. K. *Biomass Bioenergy*, **2012**, *41*, 94.
[46] Ezzatzadeh, E.; Hossaini, Z. *Nat. Prod. Res*. **2018**, *4*, 1.

[47] Khaleghi, F.; Bin Din, L.; Rostami Charati, F.; Ahmad Yaacob, W.; Khalilzadeh, M. A.; Skelton, B.; Makha. M. *Phytochem. Lett.* **2011**, *4*, 254.
[48] Ulery, L.; Graham, R. C.; Amrhein, C. *Soil Sci.* **1993**, *156*, 358.
[49] Liodakis, S.; Katsigiannis, G.; Kakali, G. *Termochim. Acta*. **2005**, *437*, 158.
[50] Misra, M. K.; Ragland, K. W.; Baker, A. J. *Biomass Bioenergy* **1993**, *4*, 103.
[51] Gerzabek, M. H. *Eur. J. Soil Sci.* **2006**, *57*, 485.
[52] Dick, D. P. *Org. Geochem.* **2006**, *37*, 1537.
[53] Radev, L. *Process Appl. Ceram.* **2010**, *4*, 15.
[54] Yildirim, A.; Mavi, A.; Kara, A. A. *J. Agric. Food Chem.* **2001**, *49*, 4083.
[55] Greeff, J.; Joubert, J.; Malan, S. F.; van Dyk, S. *Bioorg. Med. Chem.* **2012**, *20*, 809.
[56] Shimada, K.; Fujikawa, K.; Yahara, K.; Nakamura, T. *J. Agric. Food Chem.*, **1992**, *40*, 945.
[57] Yen, G. C.; Duh, P. D. *J. Agri. Food Chem.* **1994**, *42*, 629.
[58] Yildirim, A.; Mavi, A.; Kara, A. A. *J. Agric. Food Chem.*, **2001**, *49(8)*, 4083.